DOI: 10.1002/cssc.201100717

Kinetics and Reaction Engineering of Levulinic Acid Production from Aqueous Glucose Solutions

Ronen Weingarten, Joungmo Cho, Rong Xing, William Curtis Conner, Jr, and George W. Huber*[a]

We have developed a kinetic model for aqueous-phase production of levulinic acid from glucose using a homogeneous acid catalyst. The proposed model shows a good fit with experimental data collected in this study in a batch reactor. The model was also fitted to steady-state data obtained in a plug flow reactor (PFR) and a continuously stirred tank reactor (CSTR). The kinetic model consists of four key steps: (1) glucose dehydration to form 5-hydroxymethylfurfural (HMF); (2) glucose reversion/degradation reactions to produce humins (highly polymerized insoluble carbonaceous species); (3) HMF rehydration to form levulinic acid and formic acid; and (4) HMF degradation to form humins. We use our model to predict the optimal reactor design and operating conditions for HMF and levulinic acid production in a continuous reactor system. Higher temperatures (180–200 °C) and shorter reaction times (less than 1 min) are essential to maximize the HMF content. In contrast, relatively low temperatures (140–160 °C) and longer residence times (above 100 min) are essential for maximum levulinic acid yield. We estimate that a maximum HMF carbon yield of 14% can be obtained in a PFR at 200 °C and a reaction time of 10 s. Levulinic acid can be produced at 57% carbon yield (68% of the theoretical yield) in a PFR at 149 °C and a residence time of 500 min. A system of two consecutive PFR reactors shows a higher performance than a PFR and CSTR combination. However, compared to a single PFR, there is no distinct advantage to implement a system of two consecutive reactors.

Introduction

Levulinic acid (LA) is a versatile building block that for decades has been considered a basic raw chemical material owing to its high chemical reactivity.[1] This unique feature is attributed to its two highly reactive keto and carboxyl groups. This renewable biochemical can be used as a platform for the production of various high-volume organic chemicals with numerous potential industrial applications.[2] For example, levulinic acid can serve as a feedstock for the production of transportation fuels (gasoline and diesel). Esterification of levulinic acid with C_1–C_2 alcohols produces levulinic esters, which can be used as diesel additives.[3] Elliott and Frye have shown that levulinic acid can be hydrogenated in the presence of a bifunctional catalyst to produce methyl tetrahydrofuran (MTHF) in one step in relatively high yields.[4] MTHF can directly serve as a gasoline blend-stock[5] and the US Department of Energy has approved MTHF as a component of P-series-type fuels.[6]

Levulinic acid can also be converted into γ-valerolactone (GVL) via hydrogenation with molecular hydrogen or formic acid (FA).[7,8] GVL has been shown to be a sustainable liquid transportation fuel suitable of replacing ethanol in gasoline–ethanol blends.[9] Lange et al. have shown that continued hydrogenation of GVL produces valeric acid, which can be esterified with alcohols to produce a new class of cellulosic transportation fuels—valeric biofuels.[10] Blends of these valeric esters with gasoline have shown promising results in engine testing. Dumesic and co-workers have recently developed an integrated catalytic process to convert GVL to liquid alkenes (ranging from C_8 to C_{24}), which could be blended with gasoline or jet fuels.[11] Butene and carbon dioxide are initially produced by decarboxylation of GVL. The products are then fed to an oligomerization reactor where butene monomers are coupled to form condensable alkenes. A comprehensive review of levulinic acid applications is given by Alonso et al.[12]

The formation of levulinic acid from carbohydrates consists of a series of consecutive reactions, which includes a hexose triple dehydration step to produce 5-hydroxymethylfurfural (HMF) and the rehydration of HMF with two molecules of water to produce levulinic acid and formic acid. Furfuryl alcohol, a product of hemicellulose depolymerization and hydrogenation, can also serve as an alternative source of levulinic acid.[13] Levulinic acid production of above 80% can be achieved from conversion of aqueous solutions of furfuryl alcohol with hydrochloric acid.[14] Extensive studies have been reported on the conversion of biomass feedstock to levulinic acid using homogeneous catalysts, including mineral acids and metal chlorides.[15–19] An overview of levulinic acid synthesis using various feedstocks and acid catalysts is given by Girisuta,[20] as well as by Rackemann and Doherty.[21]

[a] R. Weingarten, Dr. J. Cho, Dr. R. Xing, Prof. W. C. Conner, Jr, Prof. G. W. Huber
Department of Chemical Engineering
University of Massachusetts Amherst
686 North Pleasant St. 159 Goessmann Lab
Amherst, MA 01003 (USA)
Fax: (+1) 413-545-1647
E-mail: huber@ecs.umass.edu

Supporting Information for this article is available on the WWW under http://dx.doi.org/10.1002/cssc.201100717.

One commercial process for the production of levulinic acid was developed by Biofine Incorporated (presently Biofine Renewables). The Biofine process claims to produce levulinic acid at yields higher than 70% of the theoretical (58% carbon yield), based on the hexose content of the cellulosic feedstock, in a two-reactor system.[22,23] The carbohydrate-containing feedstock is initially hydrolyzed in the first reactor, a plug flow reactor (PFR), at 210–230 °C for 13–25 s in the presence of 1–5 wt% sulfuric acid. The product, HMF, is then continuously removed and supplied to a second reactor, a continuously stirred tank reactor (CSTR), where it is further hydrolyzed at 195–215 °C for 15–30 min to produce levulinic acid. A schematic of the Biofine process is shown in Scheme 1.

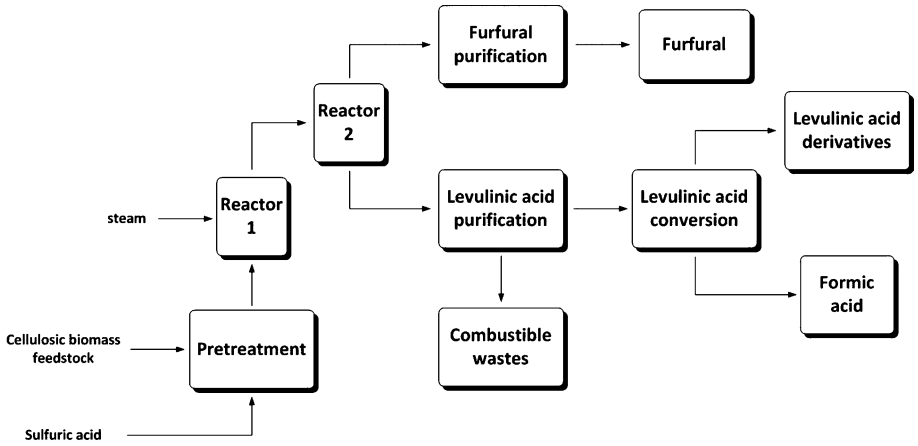

Scheme 1. The Biofine process. Adapted from Ref. [2].

Vast interest in levulinic acid applications has led to numerous kinetic studies on the decomposition of carbohydrates to produce HMF and levulinic acid. Some studies have also incorporated a hydrolysis step into their models to produce glucose from cellulose or woody biomass. The formation of undesired highly polymerized carbonaceous species (for example, humins) has been reported in the literature since the early stages of this research.[24–26] It has also been postulated that discoloration of sugar solutions is attributed to the polymerization of HMF to yield colored products of varying degrees of solubility.[27] Nonetheless, early kinetic studies only obtained kinetic parameters for the dehydration and rehydration steps leading to levulinic acid. More recent kinetic studies have incorporated undesired byproduct formation steps to enhance the accuracy of their models.[28–33]

The objective of this study is to develop a mechanistically based kinetic model for the conversion of glucose to levulinic acid in aqueous media with hydrochloric acid by fitting kinetic data collected in a batch reactor, a PFR, and a CSTR. The kinetic model will then be used to estimate the optimal reactor design and operating conditions in a continuous reactor system to maximize HMF and levulinic acid yields with a homogeneous acid catalyst.

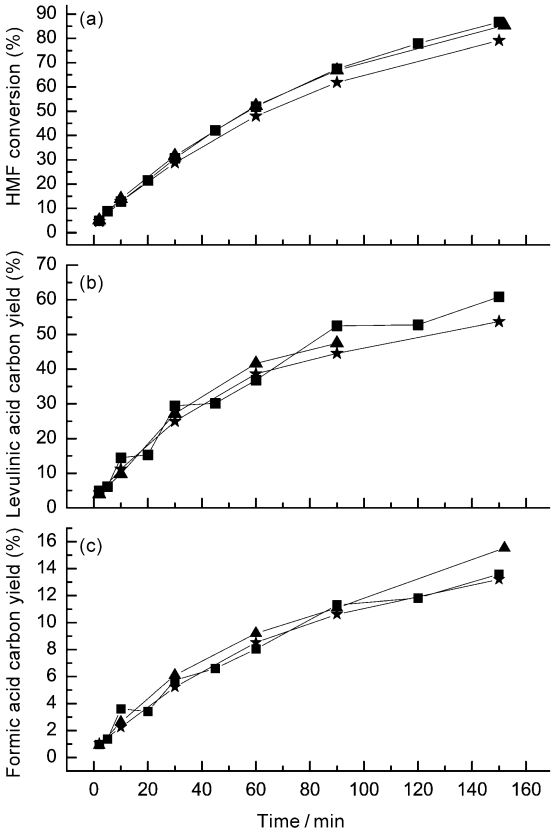

Figure 1. Aqueous-phase acid-catalyzed HMF rehydration in a stirred batch reactor. Effect of initial HMF concentration on (a) HMF conversion; (b) LA carbon yield; and (c) FA carbon yield at 130 °C and 0.1 M HCl. $[HMF]_0$ (wt%) = 4 (■), 8 (▲), 16 (★).

Results

Kinetic model for HMF rehydration

Aqueous-phase HMF rehydration experiments were carried out in a batch reactor at 120–150 °C in acidic media (0.1 M HCl) with an initial concentration of 4 wt% HMF. Similarly, additional experiments were carried out at 130 °C with initial HMF concentrations ranging between 4–16 wt% to study the effect of both feedstock and water concentration. Figure 1 shows that comparable HMF conversions and levulinic acid yields were obtained for the range of initial HMF concentrations.

HMF rehydration consists of two irreversible parallel reactions as shown in Equations (1) and (2).

$$HMF + 2\,H_2O \xrightarrow{k_3} LA + FA \quad (1)$$

$$HMF \xrightarrow{k_4} D \quad (2)$$

where D is the decomposition products (humins). The first reaction [Eq. (1)] is the rehydration of HMF with two molecules of water to produce levulinic acid and formic acid. The second reaction [Eq. (2)] is the degradation of HMF to produce humins. These proposed reactions are consistent with the mechanism proposed by Horvat et al. for levulinic acid formation from HMF.[34,35] The authors claimed that the addition of water to the 2,3-carbon positions on HMF resulted in undesired polymerization reactions, whereas the addition of water to the 4,5-carbon positions gave way to levulinic-acid formation via decarboxylation to produce formic acid. Both reactions fit equations that are pseudo first order with respect to HMF. This is in agreement with previous kinetic studies on HMF decomposition.[26,36] Furthermore, within our range of concentrations, water is considered to be in excess (zero order) in the rehydration step (see Figure 1). Some kinetic studies have also proposed an additional reaction pathway to produce humins from levulinic acid.[32,33] However, our separate studies with equimolar concentrations of levulinic acid and formic acid at 180 °C with 0.1 M HCl concluded that levulinic acid did not degrade after 120 min. This is in agreement with other studies.[26,29]

Table 1. Estimated kinetic parameters for aqueous-phase HMF conversion.[a]

Rate constants[b]	$\log_{10}$ [A/min^{-1}]	E [kJ mol^{-1}]
k_3	10.31 ± 0.71[c]	94.72 ± 5.54
k_4	15.69 ± 3.22	141.94 ± 25.72

[a] Kinetic parameters fit experimental data at: T = 120–150 °C; $[HMF]_0$ = 4–16 wt%; $[H^+]$ = 0.1 M. [b] 1st order rate parameters are lumped with acid concentration. [c] 95% confidence interval in parameter estimation.

All experimental data for HMF rehydration were fitted to the proposed kinetic model to estimate the rate parameters. Our model assumed a first order dependence with respect to the acid concentration, and the activation energies were determined for experiments carried out at a constant acid concentration of 0.1 M HCl. The best correlated values with their standard errors appear in Table 1. The estimated values of the activation energies were assumed to be independent of the acid concentration and were used for the remainder of the model fitting. On this note, it has been reported that the activation energy can be a function of acid concentration. However, this claim is valid when a reaction is governed by a slow proton transfer step.[37] It is also notable to mention that small amounts of 2-furaldehyde (furfural) were detected as a byproduct of this reaction at less than 0.04% yield. It has been reported that the formation of furfural from HMF proceeds via loss of formaldehyde.[38–41] Figure 2 shows the experimental data for HMF rehydration and levulinic-acid production with the fitted model at 0.1 M HCl.

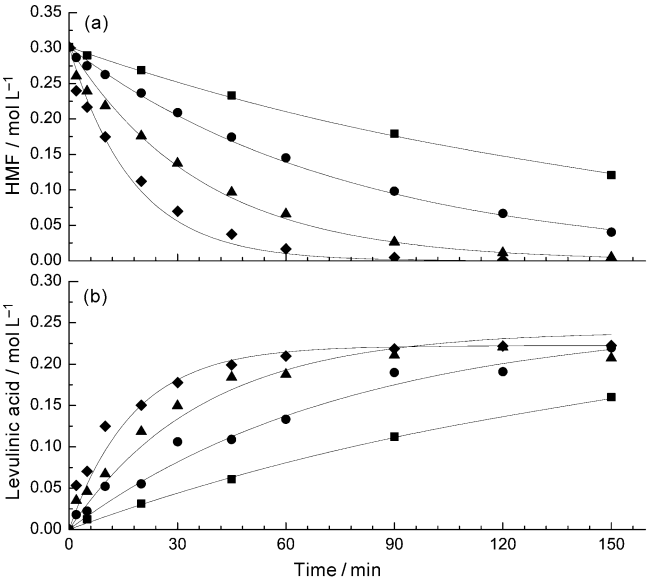

Figure 2. Aqueous-phase acid-catalyzed HMF rehydration to levulinic acid in a stirred batch reactor. Kinetic model fit for (a) HMF rehydration and (b) levulinic acid formation for 4 wt% HMF and 0.1 M HCl. T (°C) = 120 (■), 130 (●), 140 (▲), 150 (◆); Model prediction (——).

Kinetic model for glucose dehydration

Glucose dehydration experiments were carried out in a batch reactor at 140–180 °C in 0.1 M HCl with an initial glucose concentration of 10 wt%. The overall reaction scheme for the aqueous-phase levulinic acid production from glucose is shown in Scheme 2.

Glucose undergoes two irreversible parallel reactions, which consist of a triple dehydration step to produce HMF (denoted as Reaction 1), or a degradation reaction to form humins (denoted as Reaction 2). Both reactions have been reported to be pseudo first order with respect to glucose.[30] This was also confirmed with reactions that were carried out at various initial glucose concentrations ranging from 2–20 wt% at 160 °C in 0.1 M HCl. Glucose conversions, HMF yields, and levulinic acid

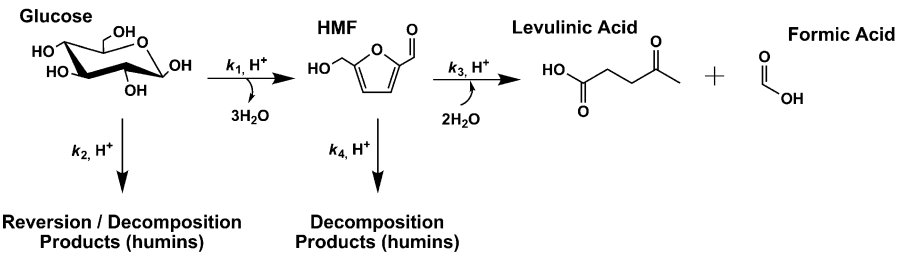

Scheme 2. Overall reaction scheme for the aqueous-phase acid-catalyzed production of levulinic acid from glucose.

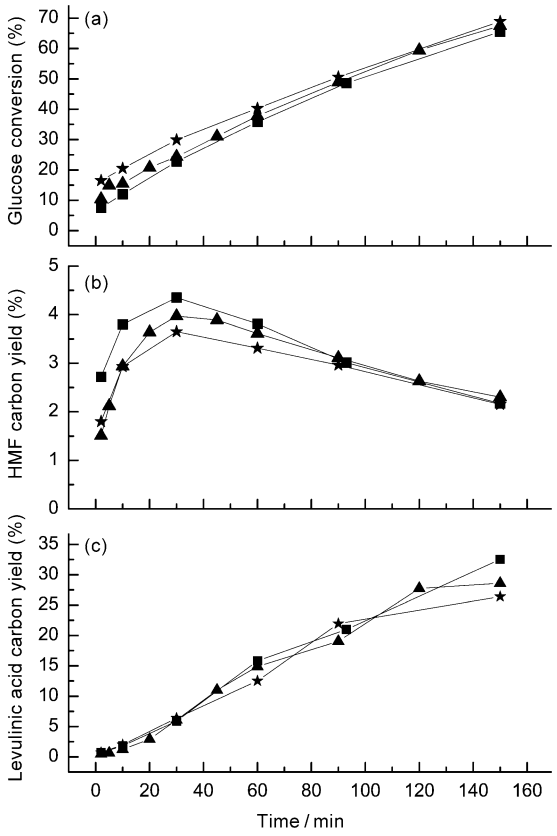

Figure 3. Aqueous-phase acid-catalyzed glucose dehydration in a stirred batch reactor. Effect of initial glucose concentration on (a) glucose conversion; (b) HMF carbon yield; and (c) LA carbon yield at 160 °C and 0.1 M HCl. $[G]_0$ (wt%) = 2 (■), 10 (▲), 20 (★).

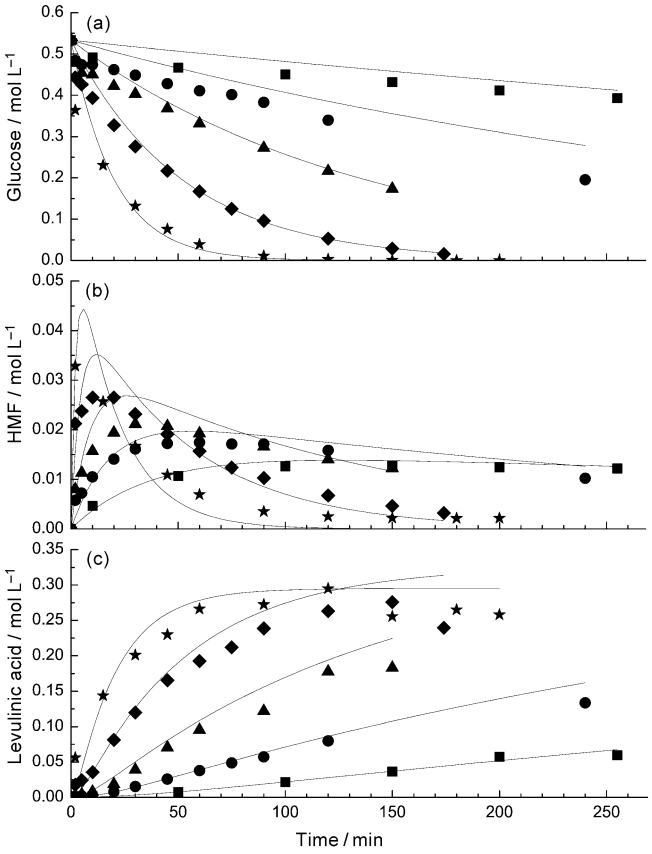

Figure 4. Aqueous-phase acid-catalyzed glucose dehydration in a stirred batch reactor. Kinetic model fit for (a) glucose dehydration; (b) HMF formation; and (c) levulinic acid formation for 10 wt% glucose and 0.1 M HCl. *T* (°C) = 140 (■), 150 (●), 160 (▲), 170 (◆), 180 (★); Model prediction (——).

yields were found to be predominantly independent of the initial glucose concentration, as illustrated in Figure 3.

The rate parameters obtained for glucose dehydration appear in Table 2. Reactions 3 and 4 (HMF rehydration and decomposition, respectively) were assumed independent of Reactions 1 and 2 (glucose dehydration and glucose decomposition, respectively). Therefore, the same rate parameters obtained for HMF rehydration (refer to Table 1) were combined with those derived for glucose dehydration to fit the experimental data to our proposed model for levulinic acid production from glucose. The experimental data for glucose dehydration, HMF, and levulinic acid production are shown in Figure 4 along with the fitted kinetic model.

Table 2. Estimated kinetic parameters for aqueous-phase glucose conversion.[a]

Rate constants[b]	$\log_{10}[A/\text{min}^{-1}]$	E [kJ mol^{-1}]
k_1	17.12 ± 0.62[c]	160.16 ± 5.15
k_2	3.33 ± 0.29	50.68 ± 2.38

[a] Kinetic parameters fit experimental data at: T = 140–180 °C; $[G]_0$ = 2–20 wt%; $[H^+]$ = 0.1 M. [b] 1st order rate parameters are lumped with acid concentration. [c] 95% confidence interval in parameter estimation.

The overall rate equations for glucose conversion are shown in Equations (3)–(5).

$$\frac{d[G]}{dt} = -(k_1 + k_2)[G] \quad (3)$$

$$\frac{d[HMF]}{dt} = k_1[G] - (k_3 + k_4)[HMF] \quad (4)$$

$$\frac{d[LA]}{dt} = k_3[HMF] \quad (5)$$

As with the HMF rehydration study, the activation energies for glucose dehydration (Reactions 1 and 2) were determined for experiments carried out at a constant acid concentration of 0.1 M HCl. Likewise, it was initially assumed that a first order dependence exists with respect to the acid concentration.

Glucose can also undergo reversion and epimerization reactions to produce oligosaccharides and anhydrosugars and fructose, respectively.[25,30,42] The reversion products are mainly disaccharides, which are formed by way of a coupling reaction of the anomeric hydroxyl group of one glucose molecule with any hydroxyl group of a second molecule.[43] It has also been suggested that the products from reversion reactions can be subject to degradation reactions, in which the disaccharides react further to form oligosaccharides.[44] Consequently, the presence of cellobiose confirmed the occurrence of reversion

reactions in this study. Levoglucosan (1,6-anhydro-β-D-glucopyranose) and fructose were also detected in the reaction samples in qualitative amounts. Fructose was present at less than 0.1% yield. Previous studies have shown that the formation of fructose from glucose in acidic solution proceeds by way of a C_2-to-C_1 intramolecular hydrogen transfer.[45] The role of the acid catalyst is to protonate the carbonyl oxygen atom to facilitate a hydride shift mechanism.[46] Similar conclusions were deduced by Davis and co-workers in their study of aqueous-phase isomerization of glucose to fructose with a solid Lewis acid catalyst.[47–49]

Hence, one theory suggests that the formation of HMF from glucose proceeds via fructose[43] and that the near-nil presence of fructose can be attributed to its high reactivity compared to glucose.[45,50] Conversely, other authors claim that glucose can be converted directly to HMF through cyclization of a 3-deoxyglucosone intermediate formed from the open-ring form of glucose.[51,52] In this respect, the relatively low conversion of glucose to HMF is caused by its low affinity to exist in the open-ring form due to stabilization of the glucose pyranose forms in aqueous solution.[53] Overall, there are two schools of thought with regard to the mechanism of HMF formation from C_6 carbohydrates. One theory postulates that the reaction proceeds by way of the acyclic 1,2-enediol intermediate.[45,54] The other takes into account a fructofuranosyl cyclic intermediate in the formation of HMF from fructose.[51,55] Recent computational studies have also reported the use of fructofuranosyl intermediates in the formation of levulinic acid and HMF from glucose and fructose, respectively.[53,56] Caratzoulas and Vlachos studied the energetics of the acid-catalyzed dehydration of fructose to HMF via the closed-ring mechanism.[57] They found that the reaction proceeds by way of intramolecular proton and hydride transfers.

Furfural was also detected as a final byproduct of the dehydration reaction of glucose, at less than 0.61% yield. As mentioned previously, it is possible that HMF is the precursor for furfural accumulation. However, some have also postulated alternative pathways to produce furfural from hexoses via a pentose unit with formaldehyde or formic acid as byproducts.[40,58,59] Incidentally, formic acid can also be produced directly from C_6 monosaccharides,[59] as well as from furfural.[60,61] Regardless, it is reasonable to assume that formic acid was produced via multiple routes in addition to the conventional pathway from HMF rehydration. Accordingly, an excess of formic acid was detected throughout the entire study relative to the kinetic model data, as depicted in Figure 5. Consequently, the LA-to-FA carbon molar ratio was lower than its stoichiometric value of five in this study.

Effect of acid concentration

Further glucose dehydration experiments were carried out at acid concentrations with 0.5 and 1.0 M HCl and temperatures between 140–180 °C. The initial glucose concentration was kept constant at 10 wt%. The kinetic model fitted to the experimental data of glucose dehydration at 0.5 and 1.0 M HCl appear in the Supporting Information (refer to Figures S1 and S2). As mentioned previously, activation energies were calculated for reactions at 0.1 M HCl and assumed to be constant for all other acid concentrations. The pre-exponential factors were calculated for each reaction step x (refer to Scheme 2) at each acid concentration, and a power law function was derived, as shown in Equation (6). This approach was similar to those used by Saeman[24] and Kuster and Temmink.[50] The best kinetics fit parameters with their standard errors are tabulated in Table 3.

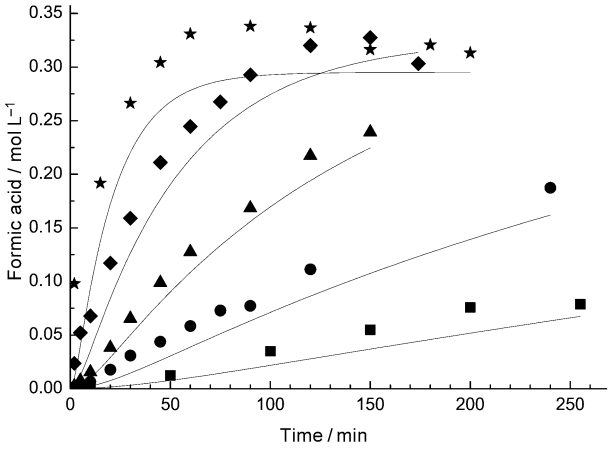

Figure 5. Aqueous-phase formic acid production from glucose in a stirred batch reactor. Comparison between experimental and kinetic model data. Feed was 10 wt% glucose and 0.1 M HCl. T (°C) = 140 (■), 150 (●), 160 (▲), 170 (◆), 180 (★); Model prediction (——).

$$A_x = A_{x,0} \times \left(H_{x,0} + [H^+]^{n_x}\right) \quad (6)$$

$A_{x,0}$, $H_{x,0}$, and n_x are correlating parameters to describe dependence of the pre-exponential factor on acid concentration. Non-catalyzed reactions were also performed at various temperatures to study the effect of glucose decomposition without HCl in the aqueous solutions. As shown in Figure 6a, the rate of glucose disappearance increased with temperature, and nearly full disappearance was reached at 180 °C after 150 min. Figure 6b reveals that the maximum attainable carbon yield of HMF is 7.5% at 180 °C after 60 min. Levulinic acid was detected only at 180 °C after 60 min, and a maximum carbon yield of 12% was obtained after 150 min. The total organic carbon (TOC) analysis confirmed that at high temperatures only 50% of the water-soluble organic carbon was accounted for. Up to 50% of the overall organic carbon went into forming insoluble humic species. This finding agrees with Figure 6c, which plots

Table 3. Estimated kinetic parameters for aqueous-phase glucose dehydration to levulinic acid with dependence on acid concentration.[a]

x	$\log_{10}\left[A_{x,0}/(M^{-n_x}\ \mathrm{min}^{-1})\right]$	E_x [kJ mol^{-1}]	$H_{x,0}$	n_x
1	18.44 ± 0.98[b]	160.16 ± 5.15	0	1.290 ± 0.062
2	3.86 ± 0.52	50.68 ± 2.38	0.29 ± 0.01	2.764 ± 0.213
3	11.50 ± 0.83	94.72 ± 5.54	0	1.176 ± 0.103
4	16.83 ± 3.43	141.94 ± 25.72	0	1.176 ± 0.114

[a] Kinetic parameters fit experimental data at: T = 140–180 °C; $[G]_0$ = 2–20 wt%; 0 M < $[H^+]$ ≤ 1.0 M. [b] 95% confidence interval in parameter estimation.

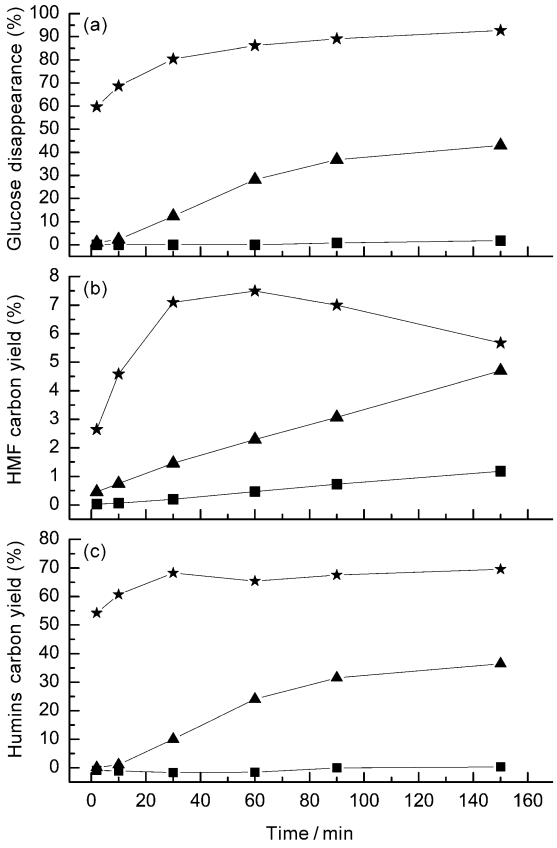

Figure 6. Aqueous-phase non-catalyzed thermal decomposition of glucose in a stirred batch reactor. T (°C) = 140 (■), 160 (▲), 180 (★). Feed was 10 wt% glucose. (a) Glucose disappearance; (b) HMF carbon yield; (c) humins carbon yield.

the total humin carbon yield. For this purpose, humins were considered non-detectable soluble and insoluble compounds.

Continuous reactor systems

The kinetic model derived above can be further used to model data from continuous reactor systems. These can be divided into two reactor types based on the mixing of the reactant—PFR and CSTR. Under steady-state operating conditions, their design equations are described as Equations (7) and (8):

$$\text{PFR}: \quad \tau = C_{i,0} \int_0^{X_i} \frac{dX_i}{-r_i} \tag{7}$$

$$\text{CSTR}: \quad \tau = \frac{C_{i,0} X_i}{-r_i} \tag{8}$$

where τ is the residence time, $C_{i,0}$ the initial concentration of species i, r_i the corresponding reaction rate, and X_i the conversion of species i. The above equations were combined with the kinetic model [Eqs. (3)–(6)] to simulate continuous production of levulinic acid. The key process variables include initial concentration of glucose, acid concentration, temperature, and residence time. The variables can be manipulated to maximize throughput, conversion of glucose, and yields of HMF and levulinic acid. Experimental studies were also carried out with a PFR and a CSTR at temperatures between 160–180 °C with 0.5 M HCl. Steady-state conditions were attained after a period corresponding to 4–5 times the residence time of the reactor. This was confirmed by sampling multiple times at each steady-state condition and taking the average value along with its standard deviation. The experimental data along with the fitted models are shown in Figure 7.

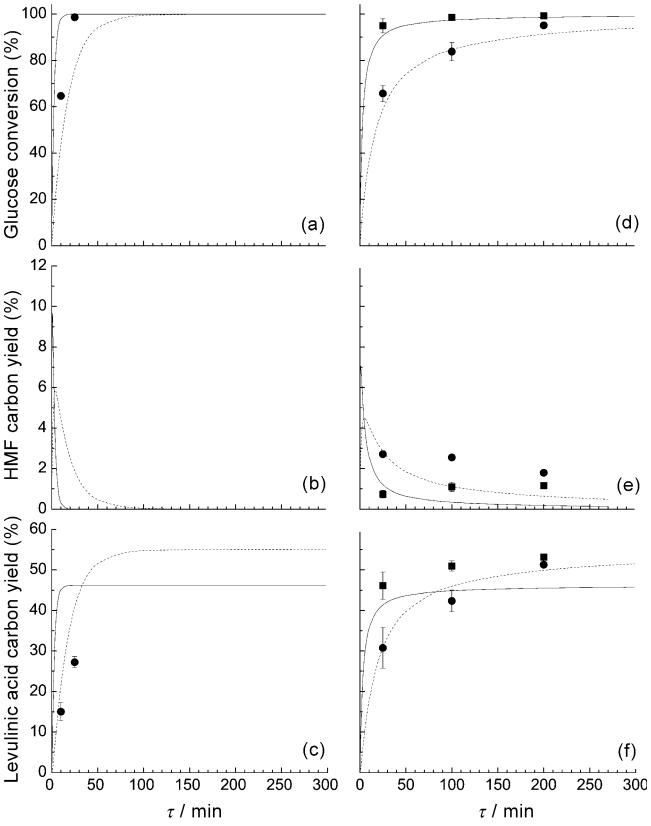

Figure 7. Aqueous-phase acid-catalyzed glucose dehydration in continuous reactors. Kinetic model fit with a single PFR (plots a, b, c) and single CSTR (plots d, e, f) for glucose conversion, HMF carbon yield, and LA carbon yield. Experimental reaction conditions: 3–5 wt% glucose and 0.5 M HCl. T (°C) = 160 (●), 180 (■); Model prediction for 160 °C (-----); Model prediction for 180 °C (——).

The kinetic model shows that the rate of glucose conversion is higher in a PFR compared to a CSTR. Likewise, maximum HMF carbon yields of 10% are obtained in a PFR at 180 °C and short residence times (less than 1 min). A maximum levulinic acid yield of 55% is obtained in a PFR at 160 °C and a residence time of 100 min. This is compared to 46% LA carbon yield obtained in a CSTR at the same temperature and residence time. As shown, there is some inconsistency between the experimental data and the theoretical model. This could be due to a number of factors, such as non-ideal mixing patterns in the reactors. From an operational point of view, challenges arise due to the formation of solid humic species in the reactors. This is predominantly encountered in the PFR, which ultimately results in high pressure drops across the reactor and reduction of the reactor volume. Therefore, only experiments at relatively

low temperatures and short residence times are currently feasible in the PFR. Conversely, the formation of solid humins has a negligible effect on the operational aspect of the CSTR and consequently harsher reaction conditions can be employed.

Discussion

Comparison with previous kinetic models

The kinetic parameters derived from our model (Table 3) are in fairly good agreement with those obtained in previous studies. The literature reports activation energies for acid-catalyzed glucose dehydration (Reaction 1) in the range 121–152 kJ mol^{-1} (see Table 4 for references). Our study reported a value of 160 kJ mol^{-1} with a 95% confidence interval of ± 5, which is in the range of previous studies. The majority of the literature values for acid-catalyzed HMF rehydration (Reaction 3) range from 95 to 111 kJ mol^{-1}. This is in agreement with our reported value of 95 ± 6 kJ mol^{-1}. Girisuta et al. claimed activation energies of 165 and 111 kJ mol^{-1} for the formation of humins from glucose and HMF, respectively.[30] For the formation of humins from glucose (Reaction 2) and HMF (Reaction 4), we obtained values of 51 ± 2 and 142 ± 26 kJ mol^{-1}, respectively. In their study of non-catalyzed glucose decomposition, Jing and Lü reported values of 136 and 109 kJ mol^{-1} for the formation of humins from glucose and HMF, respectively.[32] Wyman and Shen reported a value of 147 kJ mol^{-1} for the formation of humins from HMF.[33] The latter value agrees well with our calculated value of 142 kJ mol^{-1}. On the other hand, our derived value of 51 kJ mol^{-1} for the formation of humins from glucose does not coincide with those reported above.

A power-law approach was used to derive the reaction orders with respect to acid concentration in the rate equations (n_x in Table 3). All reactions were found to demonstrate a near first order dependence to the acid concentration, with the exception of Reaction 2 (glucose to humins), which exhibits a near third order dependence. This differs from the values reported by Girisuta et al.[30]

A plausible cause for these observed deviations lies in the methods used to develop the kinetic models. For example, unlike our model, Girisuta et al.[29,30] used a modified Arrhenius equation to determine temperature dependence of the rate constants and a rate selectivity parameter to maximize the rate of the desired reactions. They also took into account the dissociation constant of their catalyst, as they used sulfuric acid. Our model prediction has been made for a wide range of acid concentrations extended to zero acid concentration to assure systematic dependence of rate constants on the concentration of the catalyst, that is, infinite dilution, where some of the reaction rates become negligible. Table 4 summarizes the kinetic studies that appear in the literature for glucose conversion to levulinic acid.

Table 4. Proposed kinetic models for aqueous-phase acid catalyzed glucose conversion to levulinic acid.

Proposed model[a]	Reaction conditions[b]	Ea[c] [kJ mol^{-1}]	Ref.
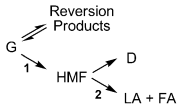	$T = 100$–150 °C [HCl] = 0.35 M $[G]_0 = 1$ wt%	$Ea_1 = 133$ $Ea_2 = 95$	[25]
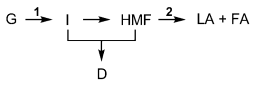	$T = 140$–250 °C $[H_2SO_4] = 0.0125$–0.4 M $[G]_0 = 5$–17 wt% $[HMF]_0 = 1$–2 wt%	$Ea_1 = 137$ $Ea_2 = 97$	[26]
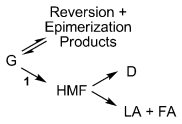	$T = 180$–224 °C $[H_2SO_4] = 0.05$–0.4 M $[G]_0 = 0.4$–6 wt%	$Ea_1 = 128$	[42]
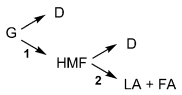	$T = 170$–230 °C $[H_3PO_4]$: pH 1–4 $[G]_0 = 0.6$–6 wt% $[HMF]_0 = 0.3$ wt%	$Ea_1 = 121$ $Ea_2 = 56$	[36]
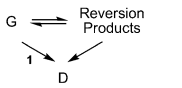	$T = 200$–230 °C $[H_2SO_4] = 0.005$–0.02 M $[G]_0 = 2$ wt%	$Ea_1 = 139$	[44]
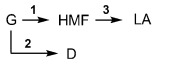	$T = 170$–190 °C $[H_2SO_4] = 0.1$–0.5 M $[G]_0 = 5$ wt%	$Ea_1 = 86$ $Ea_2 = 210$ $Ea_3 = 57$	[28]
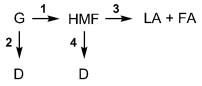	$T = 98$–200 °C $[H_2SO_4] = 0.05$–1 M $[G]_0 = 2$–15 wt% $[HMF]_0 = 1$–11 wt%	$Ea_1 = 152$ $Ea_2 = 165$ $Ea_3 = 111$ $Ea_4 = 111$	[29,30]
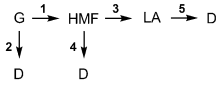	$T = 180$–280 °C non-catalyzed $[G]_0 = 1$ wt% $[HMF]_0 = 0.75$ wt% $[LA]_0 = 0.5$ wt%	$Ea_1 = 108$ $Ea_2 = 136$ $Ea_3 = 89$ $Ea_4 = 109$ $Ea_5 = 31$	[32]
	$T = 140$–180 °C 0 M < [HCl] ≤ 1.0 M $[G]_0 = 2$–20 wt% $[HMF]_0 = 4$–16 wt%	$Ea_1 = 160 \pm 5$ $Ea_2 = 51 \pm 2$ $Ea_3 = 95 \pm 6$ $Ea_4 = 142 \pm 26$	this study

[a] G = glucose; HMF = 5-hydroxymethylfurfural; LA = levulinic acid; FA = formic acid; I = intermediate; D = decomposition products (humins). [b] Units of feedstock and acid concentrations were converted for consistency. Values were rounded to the nearest unit. [c] Activation energy.

Reactor design for production of HMF and levulinic acid

The apparent rate parameters introduced here allow for theoretical calculations of HMF and levulinic acid yields. The type of reactor and its operating conditions can be modified to maximize the yields of these desired products. The kinetic model fit in Figure 7 shows that at a constant residence time higher glucose conversions and levulinic acid yields can be obtained in a PFR compared to a CSTR. Likewise, higher temperatures and short residence times are essential to maximize the HMF yield. These conditions are favored in a PFR-type reactor.

This finding also agrees with our previous work on furfural production from xylose.[62] In contrast, lower temperatures are necessary to obtain optimal levulinic acid yields. This is due to the induced HMF degradation reaction (Reaction 4) that occurs at relatively higher temperatures ($Ea_4 > Ea_3$).

The calculated HMF and levulinic acid yields are shown in Figure 8 as a function of glucose conversion for an ideal PFR and CSTR. On a conversion basis, the HMF yield is maximized in a PFR at high temperatures. This is because the dehydration step to form HMF (Reaction 1) is favored at increased temperatures due to its higher activation energy compared to the degradation step to form humins from glucose (Reaction 2). At similar feedstock conversions shorter residence times are obtained in a PFR compared to a CSTR. This shorter residence time minimizes the further decomposition of HMF and maximizes the HMF production. Calculations show that a HMF yield of 14% can be obtained at 200 °C in a PFR at 34% glucose conversion. This conversion corresponds to a residence time of 10 s.

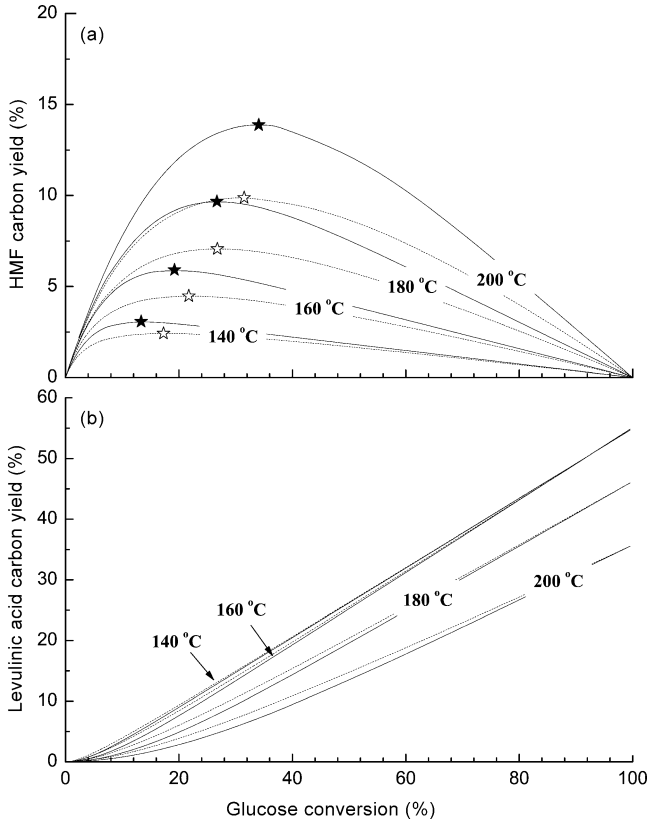

Figure 8. Continuous reactor modeling for acid-catalyzed glucose dehydration in a single continuous reactor. Calculated values for (a) HMF carbon yield and (b) LA carbon yield as a function of glucose conversion and temperature for 10 wt% glucose and 0.5 M HCl. PFR (——); CSTR (•••••). Symbols (★) and (☆) represent maximum HMF yields in a PFR and CSTR, respectively.

At equal glucose conversions, a slightly higher yield of levulinic acid can be obtained in a CSTR compared to a PFR (11.6 vs. 10.5% respectively, at 25% glucose conversion and 160 °C), as shown in Figure 8b. Lower temperatures (140–160 °C) are also favorable to maximize levulinic acid production, as these conditions minimize the formation of humins due to the relatively higher activation energy associated with Reaction 4 (humins from HMF) compared with the rehydration reaction to produce levulinic acid (Reaction 3). Longer residence times are required in a CSTR compared to a PFR to obtain equivalent glucose conversions. As shown in Figure 8b, the longer residence times achieved in a CSTR are favorable in the case of levulinic acid production, as we have shown that it does not undergo degradation reactions under the reaction conditions in this study.

This behavior agrees with those reported by Girisuta et al.[30] However, their kinetic model calculations show a bigger deviation between a CSTR and PFR, with increased glucose conversion. They report a LA carbon yield of 70% in a CSTR at 140 °C and complete glucose conversion. Our model predicts an LA carbon yield of 54% at the same temperature and conversion for both reactor types, as shown in Figure 8b. This result is comparable to that reported by Girisuta et al. in a PFR; however, there is an inconsistency with the levulinic acid yield reported in a CSTR at complete glucose conversion. To further determine the credibility of our model, we calculated the projected glucose conversion and levulinic acid yield obtained in a CSTR with the kinetic parameters reported by Girisuta et al.[30] These calculations resulted in a glucose conversion of 89.8% and an LA carbon yield of 50.4% at 160 °C, 0.5 N acid concentration, and retention time of 200 min. These results are quite similar to those reported in this study, as shown in Figure 7d and f. Experimentally, at the same reaction conditions, we obtained a glucose conversion of 95.1% and an LA carbon yield of 51.3%. Likewise, our kinetic model projected a glucose conversion of 92.0% and an LA carbon yield of 50.4%.

The calculated LA carbon yield, plotted as a function of temperature and residence time in a PFR, is shown in Figure 9. In a PFR, 56% carbon yield can be achieved at 153 °C after 200 min. The carbon yield rises to 57% with an increase in residence time to 500 min at 149 °C. However, a further increase to 1000 min shows no improvement in the results. If the residence time in the PFR decreases, then a higher temperature is required to maximize levulinic acid production. This in turn results in lower yields of levulinic acid due to the induced formation of humins from HMF (Reaction 4). The levulinic acid yield has an optimum with regard to temperature and residence time. On the one hand, HMF production from glucose (Reaction 1) is maximized at elevated temperatures ($Ea_1 > Ea_2$). Conversely, high temperatures are unfavorable for levulinic acid production from HMF (Reaction 3) due to a parallel degradation step with a higher activation energy ($Ea_4 > Ea_3$).

In addition to operating parameters, a variety of reactor configurations can be examined, including a combination of two reactors in series. Figure 10 plots the overall calculated levulinic acid yield for two reactors in series as a function of the temperature and residence time of the second reactor (T_2 and τ_2, respectively). The first reactor is a PFR, as we have shown that this reactor type is favorable to maximize levulinic acid yield. Its operational conditions were set to maximize the levulinic acid yield in the first reactor. The second reactor depicts a PFR

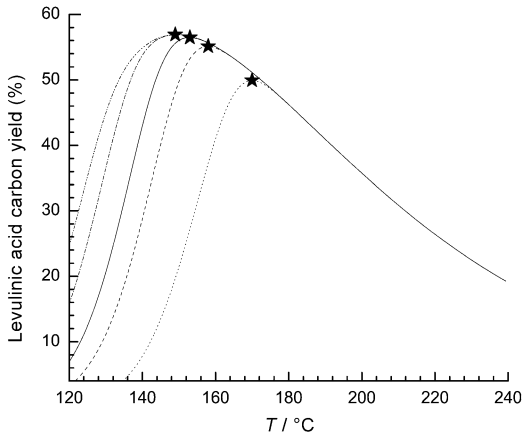

Figure 9. Continuous reactor modeling for acid-catalyzed glucose dehydration in a PFR. Calculated LA carbon yield as a function of temperature for 10 wt% glucose and 0.5 M HCl at varying residence times. τ (min) = 25 (••••), 100 (-----), 200 (——), 500 (–•–•), 1000 (—••—••). Symbol (★) represents maximum LA carbon yield.

or CSTR as shown in Figure 10a and b, respectively. As can be seen, a combination of two PFR reactors in series is preferred relative to a PFR and CSTR combination. The former gives rise to a higher levulinic acid yield (52.5 vs. 47.5%) at shorter residence times in the second reactor (55 vs. 93 min). The contour plots demonstrate that a decrease in the temperature of the second reactor subsequently requires an increase in its residence time to maintain equivalent levulinic acid yields. The combination of two PFRs in series shows nearly the same results as a single PFR. According to Figure 7, a single PFR at 160 °C and residence time of 50 min can yield 51.7% levulinic acid, which is similar to the maximum yield of 52.5% obtained with two PFRs in series at 160 °C and residence time of 60 min.

Our proposed model for levulinic acid production from glucose differs from that employed by the Biofine process. As mentioned previously, this commercial process consists of two acid-catalyzed steps: (1) hydrolysis of the lignocellulosic biomass feedstock to monosaccharides and subsequent dehydration to produce HMF; (2) rehydration of HMF to produce levulinic and formic acid. Furfural is also produced during the process. The first stage takes place in a PFR reactor between 210–230 °C within 13–25 s. The second stage consists of a CSTR reactor at temperatures between 195–215 °C and residence times of 15–30 min.

The general operating trend realized by the Biofine process agrees with our model, in that initially higher temperatures are necessary to maximize the hydrolysis/dehydration step and then lower temperatures should be employed to maximize the levulinic acid yield. However, a discrepancy arises with respect to the optimal reactor configuration. The Biofine process uses a PFR followed by a CSTR, whereas our model predicts a single PFR as the most favorable. This inconsistency could be due to the fact that, unlike the Biofine process, a biomass hydrolysis step was not included in our proposed model. This preliminary depolymerization step has a high energy barrier and requires relatively high temperatures,[24,63] which could necessitate a multi-stage process.[21] Hayes et al. have suggested that higher yields are obtained in a CSTR in the Biofine process because this reactor minimizes the "higher-order" degradation reactions, compared to the first order rehydration of HMF to produce levulinic acid.[64] Their claim differs from our proposed kinetic model, which suggests that all four of the reactions are first order with respect to the reactants [refer to Eqs. (3)–(5)]. A CSTR may also be beneficial compared to a PFR because of the operational issues associated with the formation of solid humins during the reaction. As observed in this study, it may well be easier to operate a CSTR amid the formation of solid humins compared to a PFR.

According to the Biofine process, levulinic acid production can reach carbon yields higher than 58% (70% of the theoreti-

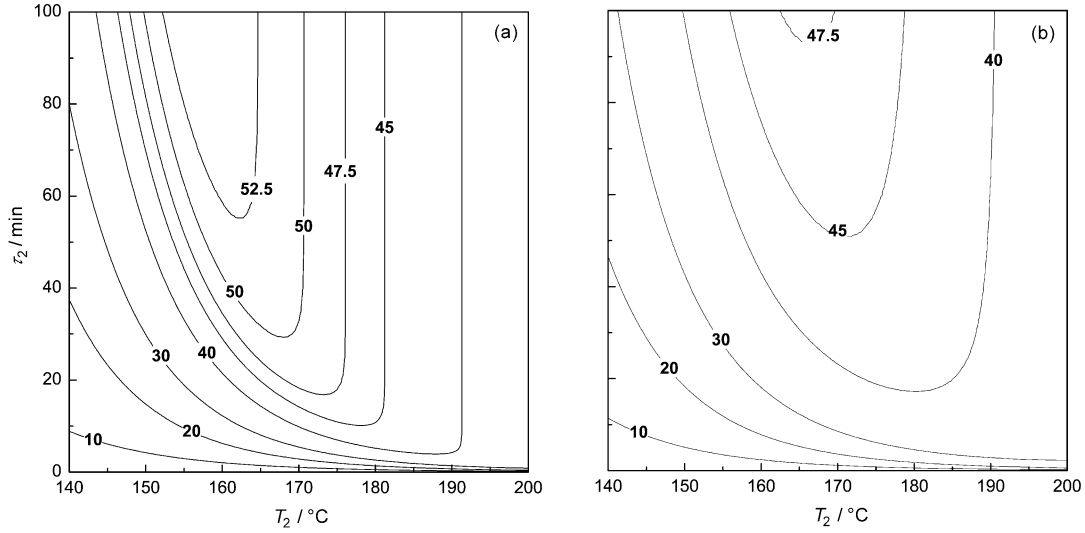

Figure 10. Continuous reactor modeling for acid-catalyzed glucose dehydration in a system of two reactors in series. Calculated total LA carbon yield as a function of the residence time (τ_2) and temperature (T_2) of the second reactor for 10 wt% glucose. For both cases the first reactor is a PFR at: $T_1 = 200$ °C, $\tau_1 = 5$ s, and 0.5 M HCl. The second reactor is (a) PFR or (b) CSTR, both at 0.5 M HCl.

cal yield) from cellulosic biomass.[22,23] Similarly, in this study we project a maximum carbon yield of 57% (68% of the theoretical yield) levulinic acid from glucose, as shown in Figure 9. Likewise, in their kinetic study of levulinic acid production from cellulose, Wyman and Shen report a maximum LA carbon yield of 50% (60% of the theoretical) at an initial 99.6 mM cellulose concentration, a 0.927 M acid concentration, and temperatures between 180–200 °C.[33]

Conclusions

In this paper we have developed a kinetic model for aqueous-phase glucose dehydration to produce 5-hydroxymethylfurfural (HMF) and levulinic acid. Our model involves four reactions. Glucose first undergoes a dehydration reaction in which three molecules of water are removed to produce HMF (Reaction 1). In a parallel step, glucose can undergo reversion and decomposition reactions to form humins, which are highly polymerized insoluble carbonaceous species (Reaction 2). Once HMF is formed, it can also undergo parallel reactions. In the presence of water, a rehydration reaction takes place with two molecules of water to produce levulinic acid and formic acid (Reaction 3). Likewise, HMF can also decompose to form humic species (Reaction 4).

The proposed kinetic model is consistent with the experimental data for batch reactions within the conditions of this study. Some inconsistency was observed with regard to the continuous reactors, predominantly with the PFR. Formation of solid humins during the reaction is the probable cause of this discrepancy. Minimizing the occurrence of humins would consequently improve the operational aspect of the continuous reactors.

Theoretical calculations have allowed us to recognize the optimal reactor configuration and operating conditions to achieve maximum HMF and levulinic acid yields. In general, higher temperatures (i.e., 180–200 °C) and short reaction times of less than 1 min are essential to maximize the HMF content. On the other hand, low temperatures between 140–160 °C and long residence times of greater than 100 min are essential for maximum levulinic acid yield.

A plug flow-type reactor (PFR)-type reactor is favorable for the aqueous-phase production of HMF and levulinic acid from glucose, as compared with a continuously stirred tank reactor (CSTR). Higher HMF yields can be obtained in a PFR at relatively shorter residence times. Likewise, compared to a PFR, a CSTR requires longer residence times to attain comparable levulinic acid yields. A maximum calculated LA carbon yield of 57%, or 68% of the theoretical yield, can be obtained in a PFR at 149 °C and a residence time of 500 min. The optimal operating conditions for HMF production are 200 °C and a reaction time of 10 s in a PFR-type reactor with a maximum attainable carbon yield from glucose of 14%. Overall, from an economical and operational point of view, there is a trade-off between the reactor temperature and residence time. Shorter residence times require higher temperatures, which can consequently jeopardize the final yield of levulinic acid. Finally, we have shown that a system of two consecutive PFRs has a higher performance than a PFR and CSTR combination. Compared to a single PFR, for the aqueous-phase levulinic acid production from glucose, there is no distinct advantage to implementing a system of two consecutive reactors.

Experimental Section

Reaction kinetics measurements

Batch reactions were carried out in a 100 mL reactor vessel provided by Parr Instrument Company, series 4560. The feedstock solutions were prepared with deionized (DI) water at the specified concentrations. Acidic solutions were prepared with HCl (Fisher Scientific). Glucose was provided by Fisher Scientific. HMF (99%) was provided by Sigma Aldrich. Levulinic acid (98%) and formic acid (98%) were provided by Acros Organics. Temperatures in the reactor were measured by a thermocouple in the solution. All reaction solutions were mixed at a maximum constant rate of 600 rpm using an internal stirrer. The temperature and stirring were controlled by a 4848 Controller provided by Parr. The reaction vessel was initially pressurized to 5.5 MPa with industrial grade helium (Airgas). Samples were taken periodically by way of a sampling port. The samples were immediately quenched in an ice water bath and filtered with a 0.2 μm syringe filter prior to analysis. The reactor was repressurized with helium after each sampling.

Continuous reactions were carried out in both a PFR and a CSTR. The PFR reactor was prepared by using a stainless steel tube of 6.35 mm outer diameter (OD). A Varian HPLC pump (Prostar 210) was used to introduce the feedstock into the reactor at flow rates ranging from 0.065–1.293 mL min^{-1}. The reactor was heated by means of a heating tape (McMaster–Carr), and insulation tape was used to minimize heat losses. A thermocouple was placed adjacent to the reactor wall to measure the temperature and was connected to a temperature controller. The reactor system was initially pressurized to 4.1 MPa with UHP grade helium (Airgas). Liquid products were recovered in a sample vessel at room temperature. The samples were filtered with a 0.2 μm syringe filter prior to analysis.

The CSTR with a 100 mL reactor vessel was modified from a Parr batch reactor, allowing continuous liquid flow in and out of the reactor. A Varian HPLC pump (Prostar 210) was used to introduce the feedstock into the reactor through a port on the reactor cap. The flow rates ranged from 0.300–2.400 mL min^{-1}. A dip tube was used as the outlet of the reactor. The temperature and stirring were controlled as described for the batch reactions. The reaction vessel was initially pressurized to 5.5 MPa with industrial grade helium (Airgas). A back-pressure regulator was used to monitor the pressure of the system. Liquid products were recovered in a sample vessel at room temperature. The samples were filtered with a 0.2 μm syringe filter prior to analysis.

Analysis

Samples were analyzed by means of HPLC with a Shimadzu LC-20AT. Carbohydrates were detected with a refractive index detector (RID-10A), and products were detected with a UV-Vis detector (SPD-20AV) at wavelengths of 210 and 254 nm. A Biorad Aminex HPX-87H sugar column was used. The mobile phase was 5 mM H_2SO_4 flowing at a rate of 0.6 mL min^{-1}. The column oven was set to 30 °C. The TOC measurements were performed with a Shimadzu TOC-VCPH Analyzer. Calibrations were performed with carbon standards supplied by SpectroPure.

Modeling

Experimental data was collected and used to compare with the proposed kinetic model to estimate rate parameters of the reaction pathways for levulinic acid production from glucose. The kinetic model for the overall reaction paths was a set of coupled ordinary differential equations (ODEs) and rate constants were correlated by the Arrhenius equation to include temperature dependence. The pre-exponential factors and activation energies were set as adjustable parameters to simultaneously correlate a complete set of concentration data for reactants and products at different temperatures (120–180 °C). The sum of absolute errors between estimated and observed values was minimized to find the best fit with the observed reaction rates of glucose dehydration and levulinic acid formation. Matlab and Athena Visual Studio (v14.0) were used for the numerical integration of ODEs and parameter estimations.

Acknowledgements

The authors gratefully acknowledge financial support from NSF-CBET (Grant 0756663) and NSF MRI (Grant 0722802). We also sincerely thank Alejandro Fernández for his contribution in the lab.

Keywords: flow reactor · glucose · homogeneous catalysis · kinetics · reaction mechanism

[1] R. Leonard, *Ind. Eng. Chem.* **1956**, *48*, 1330.
[2] J. J. Bozell, L. Moens, D. C. Elliott, Y. Wang, G. G. Neuenscwander, S. W. Fitzpatrick, R. J. Bilski, J. L. Jarnefeld, *Resour. Conserv. Recycl.* **2000**, *28*, 227.
[3] S. W. Fitzpatrick, *ACS Symp. Ser.* **2006**, *921*, 271.
[4] D. C. Elliott, J. G. Frye, US 5883266, **1999**.
[5] S. Bayan, E. Beati, *Chim. Ind.* **1941**, *23*, 432.
[6] G. W. Huber, S. Iborra, A. Corma, *Chem. Rev.* **2006**, *106*, 4044.
[7] H. Heeres, R. Handana, D. Chunai, C. B. Rasrendra, B. Girisuta, H. J. Heeres, *Green Chem.* **2009**, *11*, 1247.
[8] L. Deng, Y. Zhao, J. Li, Y. Fu, B. Liao, Q.-X. Guo, *ChemSusChem* **2010**, *3*, 1172.
[9] I. T. Horváth, H. Mehdi, V. Fabos, L. Boda, L. T. Mika, *Green Chem.* **2008**, *10*, 238.
[10] J.-P. Lange, R. Price, P. M. Ayoub, J. Louis, L. Petrus, L. Clarke, H. Gosselink, *Angew. Chem.* **2010**, *122*, 4581; *Angew. Chem. Int. Ed.* **2010**, *49*, 4479.
[11] J. Q. Bond, D. M. Alonso, D. Wang, R. M. West, J. A. Dumesic, *Science* **2010**, *327*, 1110.
[12] D. M. Alonso, J. Q. Bond, J. A. Dumesic, *Green Chem.* **2010**, *12*, 1493.
[13] F. Leger, H. Hibbert, *Can. J. Res., Sect. B* **1938**, *16*, 68.
[14] B. V. Timokhin, V. A. Baransky, G. D. Eliseeva, *Russian Chemical Reviews* **1999**, *68*, 73.
[15] W. A. Farone, J. E. Cuzens, US 6054611, **2000**.
[16] J. Y. Cha, M. A. Hanna, *Ind. Crops Prod.* **2002**, *16*, 109.
[17] Q. Fang, M. A. Hanna, *Bioresour. Technol.* **2002**, *81*, 187.
[18] L. Yan, N. Yang, H. Pang, B. Liao, *Clean Soil Air Water* **2008**, *36*, 158.
[19] L. Peng, L. Lin, J. Zhang, J. Zhuang, B. Zhang, Y. Gong, *Molecules* **2010**, *15*, 5258.
[20] B. Girisuta, University of Groningen (Groningen), *PhD thesis* **2007**.
[21] D. W. Rackemann, W. O. S. Doherty, *Biofuels Bioprod. Biorefin.* **2011**, *5*, 198.
[22] S. W. Fitzpatrick, Biofine Incorporated, US 4897497, **1990**.
[23] S. W. Fitzpatrick, US 5608105, **1997**.
[24] J. F. Saeman, *Ind. Eng. Chem.* **1945**, *37*, 43.
[25] K. R. Heimlich, A. N. Martin, *J. Am. Pharm. Assoc. Sci. Ed.* **1960**, *49*, 592.
[26] S. W. McKibbins, J. F. Harris, J. F. Saeman, W. K. Neill, *For. Prod. J.* **1962**, *12*, 17.
[27] B. Singh, G. R. Dean, S. M. Cantor, *J. Am. Chem. Soc.* **1948**, *70*, 517.
[28] C. Chang, X. Ma, P. Cen, *Chin. J. Chem. Eng.* **2006**, *14*, 708.
[29] B. Girisuta, L. P. B. M. Janssen, H. J. Heeres, *Green Chem.* **2006**, *8*, 701.
[30] B. Girisuta, L. P. B. M. Janssen, H. J. Heeres, *Chem. Eng. Res. Des.* **2006**, *84*, 339.
[31] B. Girisuta, L. P. B. M. Janssen, H. J. Heeres, *Ind. Eng. Chem. Res.* **2007**, *46*, 1696.
[32] Q. Jing, X. Lü, *Chin. J. Chem. Eng.* **2008**, *16*, 890.
[33] J. Shen, C. E. Wyman, *AIChE J.* **2012**, *58*, 236.
[34] J. Horvat, B. Klaic, B. Metelko, V. Sunjic, *Tetrahedron Lett.* **1985**, *26*, 2111.
[35] J. Horvat, B. Klaic, B. Metelko, V. Sunjic, *Croat. Chem. Acta* **1986**, *59*, 429.
[36] K. D. Baugh, P. L. McCarty, *Biotechnol. Bioeng.* **1988**, *31*, 50.
[37] P. R. Bienkowski, M. R. Ladisch, R. Narayan, G. T. Tsao, R. Eckert, *Chem. Eng. Commun.* **1987**, *51*, 179.
[38] K. Kato, T. Doihara, F. Sakai, N. Takahashi, *Kenkyu Hokoku Nippon Senbai Kosha Chuo Kenkyusho* **1966**, *108*, 361.
[39] A. Ohnishi, K. Kato, E. Takagi, *Polym. J.* **1975**, *7*, 431.
[40] R. Krishna, M. R. Kallury, C. Ambidge, T. T. Tidwell, D. G. B. Boocock, F. A. Agblevor, D. J. Stewart, *Carbohydr. Res.* **1986**, *158*, 253.
[41] G. C. A. Luijkx, F. van Rantwijk, H. van Bekkum, *Carbohydr. Res.* **1993**, *242*, 131.
[42] P. C. Smith, H. E. Grethlein, A. O. Converse, *Solar Energy* **1982**, *28*, 41.
[43] H. E. van Dam, A. P. G. Kieboom, H. van Bekkum, *Starch/Staerke* **1986**, *38*, 95.
[44] Q. Xiang, Y. Lee, R. Torget, *Appl. Biochem. Biotechnol.* **2004**, *115*, 1127.
[45] D. W. Harris, M. S. Feather, *J. Am. Chem. Soc.* **1975**, *97*, 178.
[46] J. B. Binder, A. V. Cefali, J. J. Blank, R. T. Raines, *Energy Environ. Sci.* **2010**, *3*, 765.
[47] M. Moliner, Y. Román-Leshkov, M. E. Davis, *Proc. Natl. Acad. Sci. USA* **2010**, *107*, 6164.
[48] Y. Román-Leshkov, M. Moliner, J. A. Labinger, M. E. Davis, *Angew. Chem. Int. Ed.* **2010**, *49*, 8954.
[49] E. Nikolla, Y. Román-Leshkov, M. Moliner, M. E. Davis, *ACS Catal.* **2011**, *1*, 408.
[50] B. F. M. Kuster, H. M. G. Temmink, *Carbohydr. Res.* **1977**, *54*, 185.
[51] C. Perez Locas, V. A. Yaylayan, *J. Agric. Food Chem.* **2008**, *56*, 6717.
[52] E. F. L. J. Anet, *Aust. J. Chem.* **1961**, *14*, 295.
[53] R. S. Assary, P. C. Redfern, J. R. Hammond, J. Greeley, L. A. Curtiss, *J. Phys. Chem. B* **2010**, *114*, 9002.
[54] M. Chidambaram, A. T. Bell, *Green Chem.* **2010**, *12*, 1253.
[55] M. J. Antal, W. S. L. Mok, G. N. Richards, *Carbohydr. Res.* **1990**, *199*, 91.
[56] R. S. Assary, P. C. Redfern, J. Greeley, L. A. Curtiss, *J. Phys. Chem. B* **2011**, *115*, 4341.
[57] S. Caratzoulas, D. G. Vlachos, *Carbohydr. Res.* **2011**, *346*, 664.
[58] K. Kato, H. Komorita, *Agricultural and Biological Chemistry* **1968**, *32*, 715.
[59] Z. Srokol, A.-G. Bouche, A. van Estrik, R. C. J. Strik, T. Maschmeyer, J. A. Peters, *Carbohydr. Res.* **2004**, *339*, 1717.
[60] A. P. Dunlop, *Ind. Eng. Chem.* **1948**, *40*, 204.
[61] D. L. Williams, A. P. Dunlop, *Ind. Eng. Chem.* **1948**, *40*, 239.
[62] R. Weingarten, J. Cho, W. C. Conner, G. W. Huber, *Green Chem.* **2010**, *12*, 1423.
[63] R. D. Fagan, H. E. Grethlein, A. O. Converse, A. Porteous, *Environ. Sci. Technol.* **1971**, *5*, 545.
[64] D. J. Hayes, S. Fitzpatrick, M. H. B. Hayes, J. R. H. Ross, *The Biofine Process—Production of Levulinic Acid, Furfural, and Formic Acid from Lignocellulosic Feedstocks*, Wiley-VCH, Weinheim, **2008**.

Received: November 9, 2011
Published online on ■■ ■■, 0000

*R. Weingarten, J. Cho, R. Xing, W. C. Conner, Jr, G. W. Huber**

■■ – ■■

Kinetics and Reaction Engineering of Levulinic Acid Production from Aqueous Glucose Solutions

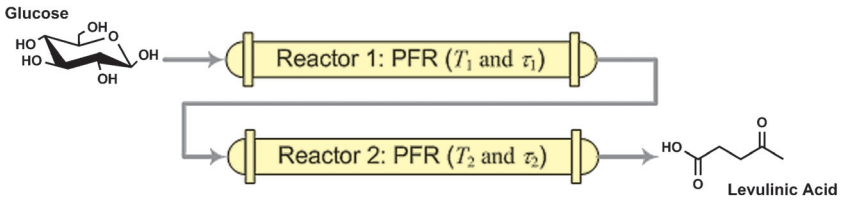

Plug wins over stirring: A plug flow reactor is preferred over a continuously stirred tank reactor for aqueous-phase production of 5-hydroxymethylfurfural and levulinic acid from glucose (estimated levulinic acid carbon yield of 57%—68% of theoretical yield). There is no distinct advantage to implementing a system of two consecutive reactors compared to a single-plug flow reactor.

